Surg Radiol Anat (2017) 39:905–910
DOI 10.1007/s00276-017-1822-2

ORIGINAL ARTICLE

# Creating vascular models by postprocessing computed tomography angiography images: a guide for anatomical education

**Figen Govsa[1] · Mehmet Asim Ozer[1] · Suzan Sirinturk[1] · Cenk Eraslan[2] · Ahmet Kemal Alagoz[3]**

Received: 29 April 2016 / Accepted: 16 January 2017 / Published online: 6 February 2017


**Abstract**
*Background* A new application of teaching anatomy includes the use of computed tomography angiography (CTA) images to create clinically relevant three-dimensional (3D) printed models. The purpose of this article is to review recent innovations on the process and the application of 3D printed models as a tool for using under and post-graduate medical education.
*Methods* Images of aortic arch pattern received by CTA were converted into 3D images using the Google SketchUp free software and were saved in stereolithography format. Using a 3D printer (Makerbot), a model mode polylactic acid material was printed.
*Results* A two-vessel left aortic arch was identified consisting of the brachiocephalic trunk and left subclavian artery. The life-like 3D models were rotated 360° in all axes in hand.
*Conclusions* The early adopters in education and clinical practices have embraced the medical imaging-guided 3D printed anatomical models for their ability to provide tactile feedback and a superior appreciation of visuospatial relationship between the anatomical structures. Printed vascular models are used to assist in preoperative planning, develop intraoperative guidance tools, and to teach patients surgical trainees in surgical practice.

✉ Figen Govsa
figen.govsa@ege.edu.tr; fgovsa@yahoo.com

1 Department of Anatomy, Ege University, 35100 Izmir, Turkey

2 Department of Radiology, Ege University, Izmir, Turkey

3 Medical Student Faculty of Medicine, Ege University, Izmir, Turkey

**Keywords** Computed tomography angiography · Three-dimentional printed model · Anatomical models · Medical education · Undergraduate education · Post-graduate education · Anatomic variation · Preoperative planning · Intraoperative guidance

## Introduction

Medical education is not confined within the medical school, but it is rather a lifelong process [2, 5, 12, 24]. All kinds of theoretical and practical experience during under and post-graduate period contribute to medical education [2, 25, 37]. Three-dimensional (3D) information plays an important role in understanding the complex structure of human anatomy in medical education [22, 33–36]. Use of 3D image displays can potentially increase the learning curve of students and increase the understanding of spatial relationships as it provides a whole representation of the patient's anatomy [18–20]. The use of 3D tools can potentially be helpful for students with lower innate spatial ability [3, 10, 22]. In recent years, new interface technologies and 3D printed models have become possible due to advanced computer technology and software [22, 27]. These printed anatomical models enable visualization and manipulation, as well as stereoscopic 3D presentation [1, 6, 21, 31].

As for the analysis of the aortic arch system, normally, it gives rise to three branches: the brachiocephalic trunk, which branches to the right subclavian and to the right common carotid arteries, the left common carotid artery and the left subclavian artery (Fig. 1) [7, 8, 14, 16, 17, 38]. Previously, the description of the six patterns of the supraaortic branches pattern and their prevalence have been gleaned from radiological and post-mortem studies (Fig. 2).

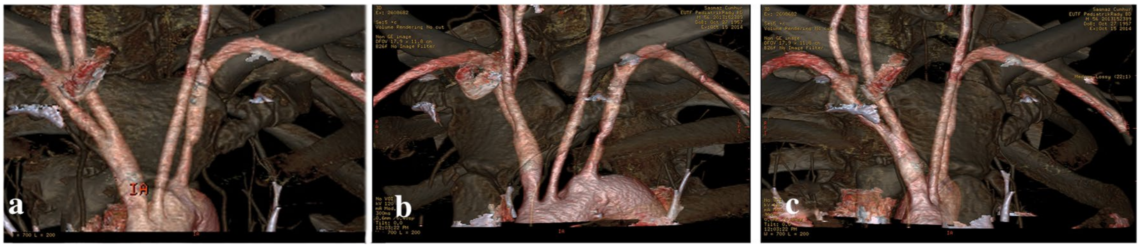


**Fig. 1** **a–c** 3D Computed tomography angiography images provide a detailed normal pattern of supraaortic arch branches originating from the left aortic arch

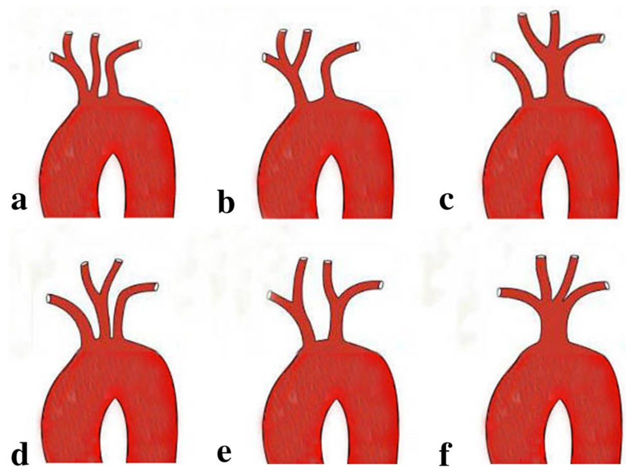


**Fig. 2** **a**–**f** Schematic presentation provides a detailed vascular map of the patterns of the branches arising from aortic arch arterial tree

Descriptions of the supraaortic arch patterns in undergraduate education were based on analyzing the structure; the clinical appliance of the essential medical knowledge is evaluated more extensively (Fig. 2a–f) [26, 39].

The production of models was obtained by high-resolution CTA and 3D printing technologies.

The aim of this study was, first, to present the anatomical variations of the aortic arch and the supraaortic arteries and to teach the formation of one-to-one direct modeling following CTA imaging and printing. Second, it targeted stressing the radiological and surgical significance of the variations based on the obtained anatomical and radiological data. The study also aimed at an innovative teaching technique approach for the undergraduate and post-graduate medical students by applying the use of imaging and printing technologies during the course of their teaching in anatomy.

## Materials and methods

The printed models of the supraaortic arch were created using 64-slice CTA data provided by the Department of Radiology, University of Ege (Fig. 3a–c). The CTA scan was performed on a 64 detector 128 sliced CT scanner (Siemens Somatom Definition AS, Siemens Medical Systems, Erlangen, Germany). The scanning was triggered by the CT technologist on the basis of contrast enhancement in the aortic arch following administration of 120 mL of iohexol with a concentration of 350 mg I/mL (Omnipaque 350; GE Healthcare, Princeton, NJ) at a rate of 4–5 mL/s. Imaging parameters include 0.6-mm section thickness, 140 kV, 250 mA, 1-s per rotation, 10–20 s to acquire images from the aortic arch to the vertex. The CTA source images were postprocessed to create contiguous coronal and sagittal reformatted images using a work station (Siemens Leonardo Workstation, Erlangen, Germany) after image reconstruction of a 2-mm section thickness, maximum intensity projection images, volume-rendered 3D images, and curved

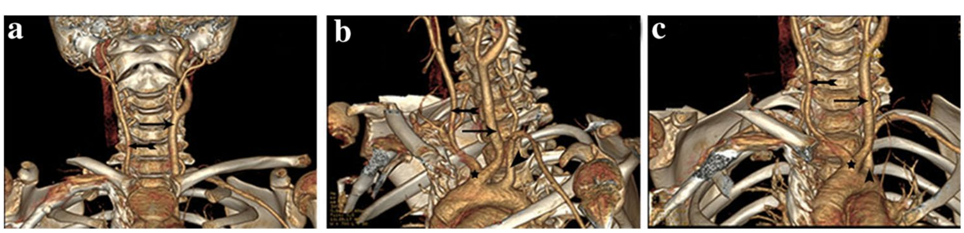


**Fig. 3** **a–c** Multislice 3D computed tomographic angiographic images of bovian type of aortic arch. The *left* common carotid artery (*arrow*) shares a origin site (*star*) with the brachiocephalic trunk. The *left* subclavian artery pointed by *arrow head* and *right* internal carotid artery indicated by *tailed arrows*

planar reformatted images of the bilateral common and internal carotid arteries. The typical dose-length product for the head and neck CTA was 2200 mGy-cm. Medical image files were in a DICOM format and were exported in image format (TIFF) files with known pixel separations. Using free software (Google SketchUp), rapid prototype bovian type of the supraaortic arch model was created. One set of models of the vascular system of the supraaortic arch were created using the volume rendering technique, based on tissue density, using CTA data (505 axial slices), and selecting density thresholds of arteries for volume segmentation (Fig. 3). The 3D CTA used for the fabrication of 3D vascular models was obtained with a slice thickness of 2 mm, to ensure high accuracy and precision. The CT data were transferred into medical image processing software (e.g., Mimics; Materialise NV, Belgium) to construct a 3D computer-aided design model. The model was saved in stereolithography file format (Fig. 4). A physical model of the processed 3D digital model was created using 3D printer Makerbot (Fig. 5). Material used was polylactic acid.

**Fig. 5** 3D printer Makerbot

## Results

Direct branches of the aortic arch are also known as the primary or the supraaortic arteries. Bovian type of the supraaortic arch pattern is the aortic arch with two branches. The first branch is the common trunk which is divided into right subclavian, right common carotid, left common carotid, and the second branch as left subclavian (Fig. 1). These structures included the aortic arch, brachiocephalic trunk, subclavian arteries, common carotid arteries, internal carotid arteries, and external carotid arteries (Fig. 6a–c). The actual model can be rotated 360° at any angle and magnified at any size for learners. Geometrical vascular anomalies can be more clearer. All reconstructed 3D printed models described here can be displayed in 3D presentation in a life-like specimen. It remains a true anatomical representation. The external shape of the aortic arch and its major branches and their dimensions are measurable. The angle formed by the aortic arch and the coronal plane was an average of 62.2° (range 30–90) and the three major branches originated from the initial third of the anterior length of the aortic arch (Fig. 6). The 3D preoperative model demonstrated the exact anatomy to understand the variable configuration in space. It also supplied us with information regarding the size of the appropriate stent graft the localization of the sealing zones.

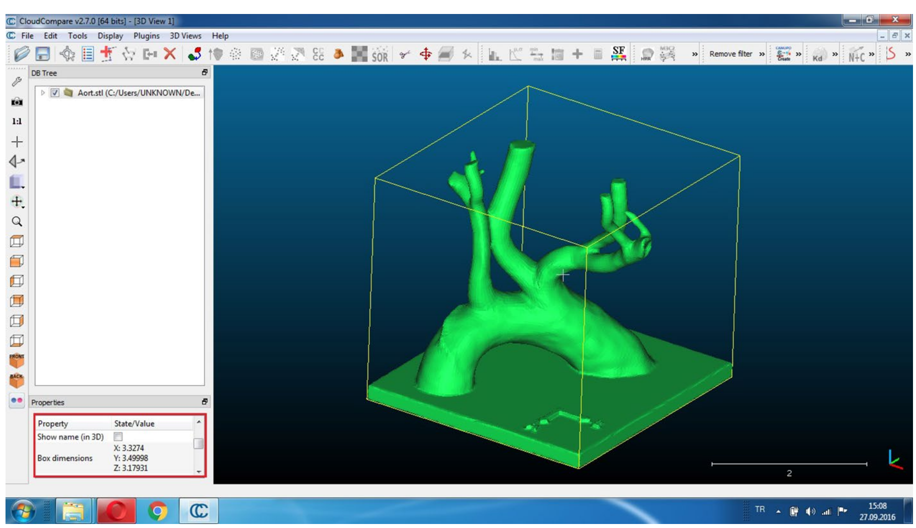


**Fig. 4** Dimensions of *X*, *Y*, and *Z* for 3-D printed models

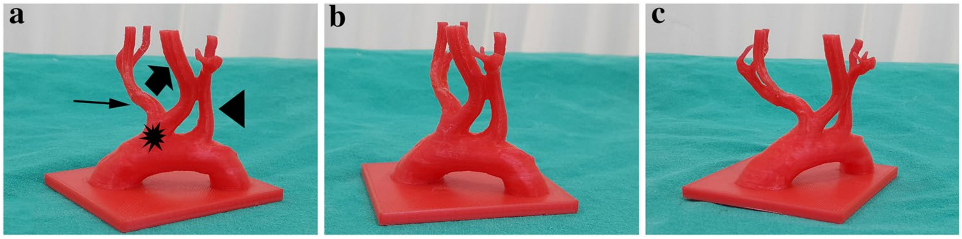


**Fig. 6** **a–c** Frontal view, side view printed three-dimensional model of the nature aortic arch including bovin type can be allowed of inspection from all angles. The *left* common carotid artery (*big arrow*) originates from the brachiocephalic trunk (*star*), close to the *left* subclavian artery (*head arrow*), *right* common carotid artery, and right subclavian artery (*slim arrow*)

## Discussion

In the current research, the use of the CTA was explored to create 3D printed models of the supraaortic arteries for geometrical vascular anomalies teaching [1, 14, 17, 19, 21, 23, 27, 35, 36]. For example, using these combined models, students are able to trace the path of supraaortic arteries visually. The model created here is the ability to place 3D vascular anatomy into the context of individual CTA slices (Fig. 6). Using this feature, students are able to visualize the bovian type of the supraaortic aortic arch design (Fig. 6); this is a point that is often confused by students via the traditional learning.

A common arterial trunk, the truncus arteriosus, arises from the primitive heart and is divided into six paired arches. The six pairs of aortic arches are a series of vessels that connect on each side the aortic sac with the corresponding dorsal aorta. At a later developmental stage, the aortic arches are both reduced in number and extensively transformed, and finally, an asymmetric blood supply system is achieved. During the third week of pregnancy, these dorsal aortae fuse caudally into a single descending aorta at the fourth thoracic vertebral level [30, 34, 38]. The first, second, and the fifth arches then regress. The third arches form the carotid arteries. The fourth arch on the right forms the brachiocephalic and right subclavian artery, whilst on the left, this forms the left subclavian artery, and the aortic arch proper, which subsequently joins the descending aorta beyond (Fig. 7).

The previous researchers reported that the variations of the aortic sac and the branchial artery system, from an embryologic standpoint can be explained by the disappearance of normally persisting vessels or from the persistence of channels that normally disappear; however, reasons for subtle variations are not understood (Fig. 7) [7–14, 32]. In this case report, we present a case of the left common carotid artery arising from the brachiocephalic trunk and absence of the main branches of the right subclavian artery in her angiographic imaging findings. The findings show that the cases whose brachiocephalic trunk and left common carotid artery originated together are the most prevalent type of variation, and the remaining cases of the variation showing either the left carotid artery originating from the aortic arch together with the brachiocephalic trunk, or that the left carotid artery originated directly from the brachiocephalic trunk. However, variations leading to the compression of the trachea and oesophagus may cause clinically significant symptoms. Every patient is unique and, therefore, should be embraced individually prior to surgical intervention [14, 39]. The aortic arch changes shape with advancing age or longstanding hypertension and this group has also undertaken the morphometric measurements of the arch branches, including the angles of origin and distance of origins from each branch. Using such data has led to the description of types of aortic arch as the angles between branch vessels become more acute, and the origin of the brachiocephalic trunk moves anteriorly.

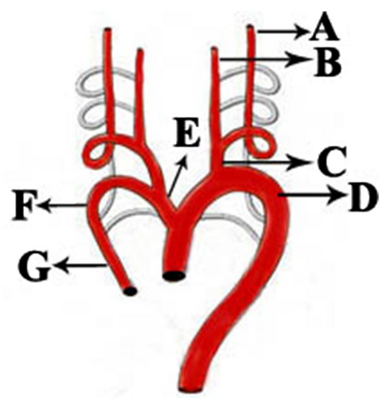


**Fig. 7** During the 6th to 8th week, the primitive aortic arch pattern is transformed into adult arterial mapping. The first, second, and fifth pairs of the aortic arches disappear (*grey colour*), while the third, fourth, and sixth pairs of aortic arches have their branches (*red colour*). Internal carotid artery (*A*), external carotid artery (*B*), common carotid artery (*C*), arch of aorta (*D*), brachiocephalic trunk (*E*), right subclavian artery (*F*), and right dorsal aorta (*G*). (Color figure online)

### Undergraduate education

The students are also reminded of the variability of human anatomy and its surgical relevance, showing the importance of personalized procedures—namely that each patient has his individual anatomy [13, 15, 28, 29]. 3D printed anatomical models can serve as accurate, tactile visualization tools, and surgical simulation devices [4, 32]. They can be utilized to reproduce complex, patient-unique anomalies, or pathologies that facilitate the surgical trainees to preoperatively predict the potential intraoperative challenges and postoperative outcomes and aid in their learning [35, 36].

### Post-graduate education

Using modeling in post-graduate education helps scientists to reach a higher level of knowledge on a variety of topics, including normal structure, embryology, the underlying congenital or acquired cause of the variational structure differences, the geometrical structure of the supraaortic arch pattern, and the distance among each pattern and the angle points [32]. The course and the variation of the brachiocephalic trunk originating from the aortic arch of life-like models can be examined (Fig. 5). Since these models are exactly the same as the human, the vascular diameter, the distance between the vessels, and similar geometrical calculations can be studied easily.

Creating the 3D printing models can reduce both the operation time, exposure to general anesthetic, decrease in blood loss, and lessen wound exposure [13, 18, 21]. Tangible 3D models allow preoperative identification and help in the selection of the appropriate surgical management and improve surgical skills of the young surgeons [3, 4, 6, 9, 12]. The models have been evaluated by the patients for their usefulness in helping to understand their illness. The patients reported that the models aid in understanding the anatomy, pathology, and the surgical risks [24, 25].

Individualized treatment approaches, customizability of 3D printing, can transform the manufacturing of patient-specific catheter to being widely accessible and affordable. 3D printed custom prostheses lead to improved clinical outcomes, such as a reduction in the length of surgery, reduced exposure to anesthetics, and a decreased risk of complications like infections. Besides their value for planning, orientation, and simulation, we believe that the life-like models are helpful for demonstrating complex procedures to the patients, colleagues, and the students [7, 8, 14].

## Conclusion

In conclusion, this study shows that the curricular innovation proposed, by combining medical imaging, 3D print technologies, and classical anatomical knowledge, is feasible with dedicated students. The anatomical vascular models obtained showed good qualitative and quantitative correlation with the authentic anatomy. Because of the cost and practicality issues, the aortic arch models can only be used for educational purposes. A collection of models and corresponding radiological images of interesting or complex case studies can be assembled to help trainees gain valuable learning experience.

#### Compliance with ethical standards

**Conflict of interest** The authors have no conflicts of interest to declare.

**Ethical standard** Ethical approval is not required for studies of this nature at our institution. All data were anonymised at source. The experiment complies with the current laws of the country in which they were performed.

## References

1. Adams CM, Wilson TD (2011) Virtual cerebral ventricular system: an MR based three-dimensional computer model. Anat Sci Educ 4:340–347
2. Anderson P, Chapman P, Ma M, Rea P (2014) Real-time medical visualization of human head and neck anatomy and its applications for dental training and simulation. Curr Med Imag Rev 9:298–308
3. Brewer DN, Wilson TD, Eagleson R, de Ribaupierre S (2012) Evaluation of neuroanatomical training using a 3D visual reality model. Stud Health Technol Inform 173:85–91
4. Brown PM, Hamilton NM, Denison AR (2012) A novel 3D stereoscopic anatomy tutorial. Clin Teach 9:50–53
5. Choi-Lundberg DL, Low TF, Patman P, Turner P, Sinha SN (2015) Medical student preferences for self-directed study resources in gross anatomy. Anat Sci Educ 9:150–160
6. Cui D, Lynch JC, Smith AD, Wilson TD, Lehman MN (2015) Stereoscopic vascular models of the head and neck: A computed tomography angiography visualization. Anat Sci Educ 9:179–185
7. Ergun E, Simsek B, Kosar PN, Yilmaz BK, Turgut AT (2012) Anatomical variations in branching pattern of arcus aorta: 64-slice CTA appearance. Surg Radiol Anat 35:503–509
8. Ergun O, Tatar IG, Durmaz HA, Birgi E, Hekimoglu B (2014) A case of a rare aortic arch variation: the avian form. JBR-BTR 97:349
9. Fasel JH, Aguiar D, Kiss-Bodolay D, Montet X, Kalangos A, Stimec BV, Ratib O (2015) Adapting anatomy teaching to surgical trends: a combination of classical dissection, medical imaging, and 3D-printing technologies. Surg Radiol Anat 38:361–367
10. Foo JL, Martinez-Escobar M, Juhnke B, Cassidy K, Hisley K, Lobe T, Winer E (2013) Evaluating mental workload of two-dimensional and threedimensional visualization for anatomical structure localization. J Laparoendosc Adv Surg Tech 23:65–70
11. Gur Y (2014) Additive manufacturing of anatomical models from computed tomography scan D data. Mol Cell Biomech 11:249–258
12. Hilbelink AJ (2009) A measure of the effectiveness of incorporating 3D human anatomy into an online undergraduate laboratory. Br J Educ Technol 40:664–672

13. Hosokawa S, Mineta H (2010) Tortuous internal carotid artery presenting as a pharyngeal mass. J Laryngol Otol 124:1033–1036
14. Jakanani GC, Adair W (2010) Frequency of variations in aortic arch anatomy depicted on multidetector CT. Clin Radiol 65:481–487
15. Kapakin S (2016) The paranasal sinuses: three-dimensional reconstruction, photo-realistic imaging, and virtual endoscopy. Folia Morphol (Warsz) 75:326–333
16. Karabulut O, Iltimur K, Cudi Tuncer M (2010) Coexisting of aortic arch variation of the left common carotid artery arising from brachiocephalic trunk and absence of the main branches of right subclavian artery: a review of the literature. Rom J Morphol Embryol 51:569–572
17. Karacan A, Turkvatan A, Karacan K (2013) Anatomical variations of aortic arch branching: evaluation with computed tomographic angiography. Cardiol Young 24:485–493
18. Knox K, Kerber CW, Singel SA, Bailey MJ, Imbesi SG (2005) Rapid prototyping to create vascular replicas from CT scan data: making tools to teach, rehearse, and choose treatment strategies. Catheter Cardiovasc Interv 65:47–53
19. Knox K, Kerber CW, Singel SA, Bailey MJ, Imbesi SG (2005) Stereolithographic vascular replicas from CT scans: choosing treatment strategies, teaching, and research from live patient scan data. AJNR Am J Neuroradiol 26:1428–1431
20. Kong X, Nie L, Zhang H, Wang Z, Ye Q, Tang L, Li J, Huang W (2016) Do three-dimensional visualization and three-dimensional printing improve hepatic segment anatomy teaching? A randomized controlled study. J Surg Educ 73:264–269
21. Lim KH, Loo ZY, Goldie SJ, Adams JW, McMenamin PG (2015) Use of 3D printed models in medical education: A randomized control trial comparing 3D prints versus cadaveric materials for learning external cardiac anatomy. Anat Sci Educ 9:213–221
22. Luursema JM, Verwey WB, Kommers PAM, Annema JH (2008) The role of stereopsis in virtual anatomical learning. Interact Comput 20:455–460
23. Marchenko Y, Volkau I, Nowinski WL (2009) Vascular editor: from angiographic images to 3D vascular models. J Digit Imaging 23:386–398
24. Marro A, Bandukwala T, Mak W (2016) Three-Dimensional printing and medical imaging: A review of the methods and applications. Curr Probl Diagn Radiol 45:2–9
25. Martin CM, Roach VA, Nguyen N, Rice CL, Wilson TD (2013) Comparison of 3D reconstructive technologies used for morphometric research and the translation of knowledge using a decision matrix. Anat Sci Educ 6:393–403
26. Natsis KI, Tsitouridis IA, Didagelos MV, Fillipidis AA, Vlasis KG, Tsikaras PD (2008) Anatomical variations in the branches of the human aortic arch in 633 angiographies: clinical significance and literature review. Surg Radiol Anat 31:319–323
27. Nguyen N, Wilson TD (2009) A head in virtual anatomy: development of a dynamic head and neck model. Anat Sci Educ 2:294–301
28. Ogden KM, Aslan C, Ordway N, Diallo D, Tillapaugh-Fay G, Soman P (2015) Factors affecting dimensional accuracy of 3-D printed anatomical structures derived from CT data. J Digit Imaging 28:654–663
29. Petersson H, Sinkvist D, Wang C, Smedby O (2009) Web-based interactive 3D visualization as a tool for improved anatomy learning. Anat Sci Educ 2:61–68
30. Pfeiffer J, Becker C, Ridder GJ (2015) Aberrant extracranial internal carotid arteries: New insights, implications, and demand for a clinical grading system. Head Neck 38:E687–E693
31. Pujol S, Baldwin M, Nassiri J, Kikinis R, Shaffer K (2016) Using 3D modeling techniques to enhance teaching of difficult anatomical concepts. Acad Radiol 23:507–516
32. Schmauss D, Haeberle S, Hagl C, Sodian R (2014) Three-dimensional printing in cardiac surgery and interventional cardiology: a single-centre experience. Eur J Cardiothorac Surg 47:1044–1052
33. Tam MD (2010) Building virtual models by postprocessing radiology images: A guide for anatomy faculty. Anat Sci Educ 3:261–266
34. Tam MD, Laycock SD, Brown JR, Jakeways M (2013) 3D printing of an aortic aneurysm to facilitate decision making and device selection for endovascular aneurysm repair in complex neck anatomy. J Endovasc Ther 20:863–867
35. Tam MD, Latham T, Brown JR, Jakeways M (2014) Use of a 3D printed hollow aortic model to assist EVAR planning in a case with complex neck anatomy: potential of 3D printing to improve patient outcome. J Endovasc Ther 21:760–762
36. Tam MD, Latham TR, Lewis M, Khanna K, Zaman A, Parker M, Grunwald IQ (2016) A pilot study assessing the impact of 3-D printed models of aortic aneurysms on management decisions in EVAR Planning. Vasc Endovascular Surg 50:4–9
37. Temkin B, Acosta E, Malvankar A, Vaidyanath S (2006) An interactive threedimensional virtual body structures system for anatomical training over the internet. Clin Anat 19:267–274
38. Vučurević G, Marinković S, Puškaš L, Kovačević I, Tanasković S, Radak D, Ilić A (2013) Anatomy and radiology of the variations of aortic arch branches in 1,266 patients. Folia Morphol (Warsz) 72:113–122
39. Wilasrusmee C, Suvikrom J, Suthakorn J, Lertsithichai P, Sitthiseriprapip K, Proprom N, Kittur DS (2008) Three-dimensional aortic aneurysm model and endovascular repair: an educational tool for surgical trainees. Int J Angiol 17:129–133